

## Pauli tomography: complete characterization of a single qubit device

A. Mazzei<sup>1</sup>, M. Ricci<sup>1</sup>, F. De Martini<sup>1,\*</sup>, and G. M. D'Ariano<sup>2</sup>

<sup>1</sup> Dipartimento di Fisica and Istituto Nazionale per la Fisica della Materia Università di Roma “La Sapienza”, 00185 Roma, Italy

<sup>2</sup> Istituto Nazionale per la Fisica della Materia and Dipartimento di Fisica “Alessandro Volta” dell’Università, Via Bassi 6, 27100 Pavia, Italy

Received 10 May 2002, accepted 17 May 2002

Published online 30 April 2003

We present the first full experimental characterization of a single-qubit device. This method uses a Pauli Process Tomography at the output of the device and needs only a single entangled state at the input, which works as all possible input states in quantum parallel. The method can be easily extended to any  $n$ -qubits processing device.

### 1 Introduction

The marriage of quantum physics and information technology, originally motivated by the need for miniaturization, has recently opened the way to the realization of radically new information-processing devices, with the possibility of guaranteed secure cryptographic communications, and tremendous speedups of some complex computational tasks. Among the many problems posed by the new information technology (1) there is the need of characterizing the new quantum devices, making a complete identification and characterization of their functioning. As we shall see, quantum mechanics provides us with a powerful tool to achieve the task easily and efficiently: this tool is the so called *quantum entanglement*, the basis of the quantum parallelism of the future computers. We present here the first full experimental quantum characterization of a single-qubit device.

How do we usually characterize the operation of a device? Actually, we are interested just in linear devices, since quantum dynamics is intrinsically linear. Any linear device, either quantum or classical (examples are: an optical lens or a good amplifier), can be completely described by a *transfer matrix* which gives the output vector by matrix-multiplying the input vector. In quantum mechanics the inputs are density operators  $\rho_{\text{in}}$  and the role of the transfer matrix is played by the so called *quantum operation* [2] of the device, that here we will denote by  $E$ . Thus the output state  $\rho_{\text{out}}$  is given by the quantum operation applied to the input state as follows:

$$\rho_{\text{out}} = \frac{E(\rho_{\text{in}})}{\text{Tr}[E(\rho_{\text{in}})]} \quad (1)$$

and the normalization constant  $\text{Tr}[E(\rho_{\text{in}})]$  is also the probability of occurrence of the transformation  $E$ , when there are other possible alternatives, such as when we consider the state transformation due to a measuring device for a given outcome.

Now the problem is: how to reconstruct the form of  $E$  experimentally? One would be tempted to adopt the conventional method [1] of running a *basis* of all possible inputs, and measuring the corresponding

\* Corresponding author E-mail: francesco.demartini@uniroma1.it

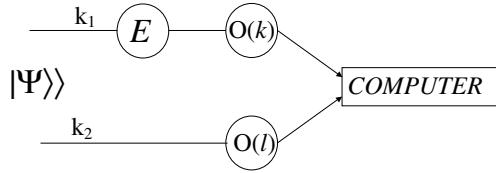


**Fig. 1** General experimental scheme of the method for the tomographic estimation of the quantum operation of a single qubit device. Two identical quantum systems, e.g. two optical beams as in the present experiment, are prepared in an entangled state  $|\Psi\rangle$ . One of the systems undergoes the quantum operation  $E$ , whereas the other is left untouched. At the output one makes a quantum tomographic estimation, by measuring jointly two observables from a quorum  $\{O(l)\}$ . In the present experiment the quorum is represented by the set of Pauli operators.

outputs by *quantum tomography* [3]. However, since the states  $\rho$  are actually operators, not vectors, in order to get all possible matrix elements we would need to run a complete orthogonal basis of quantum states  $|n\rangle$  along with their linear combination  $2^{\frac{1}{2}}(|n'\rangle + i^k |n''\rangle)$ , with  $k = 0, 1, 2, 3$  and  $i$  denoting the imaginary unit (this is a simple consequence of the polarization identity). However, the availability of such a set of states in the laboratory is, by itself, a very hard technological problem (states with a precise varying number of photons and, even worst, their superposition, are still a dream for experimentalists).

The quantum parallelism intrinsic of entanglement now comes to help us, running all possible input states in parallel by using only a single entangled state as the input! This was first shown in [4]. Hence, we don't need to prepare a complete set of states, but just one entangled state, a state commonly available in modern quantum optical laboratories!

## 2 Pauli tomography

Assume for simplicity, and with no loss of generality, that the entangled state spans a 4-dimensional Hilbert space  $H_1 \otimes H_2$ , each space  $H_i$  of dimension  $d = 2$ . The input entangled state,

$$|\Psi\rangle = \sum_{nm} \Psi_{nm} |nm\rangle \tag{2}$$

expressed in terms of the basis vectors  $|n\rangle \otimes |m\rangle = |nm\rangle$  of the two spaces  $H_i (i = 1, 2)$  is used as shown in Fig. 1 where the entangled systems consist of two single-mode optical beams. The key feature of the method implies that only one of the two systems, say system  $i = 1$ , is input into the *unknown* device  $E$ , whereas the other is left untouched. This setup leads to the output state  $R_{\text{out}}$ , which in tensor notation writes as follows

$$R_{\text{out}} = E \otimes I |\Psi\rangle \langle\langle\Psi|, \tag{3}$$

where  $I$  denotes the identical operation. It is a result of linear algebra that  $R_{\text{out}}$  is in one-to-one correspondence with the quantum operation  $E$ , as long as the state  $|\Psi\rangle$  is full-rank, i.e. it has non-vanishing components on the whole state-space of each system, such as, for instance, a so called maximally entangled state. Full-rank entangled states can be easily generated by Spontaneous Parametric Down Conversion of the vacuum state, as in the experiment reported here. Note that by this method the problem of availability of all possible input states is solved: we just need a single entangled state  $|\Psi\rangle$ , which works as all possible inputs in a sort of quantum parallelism!

Now, how to characterize the entangled state  $R_{\text{out}}$  at the output? We obviously need to perform many measurements on an ensemble of equally prepared quantum systems, since, due to the *no-cloning theorem* [5] we cannot determine the state of a single system [6]. For this purpose a technique for the full determination

of the quantum state has been introduced and developed since 1994. The method named *Quantum Tomography* [3] has been initially introduced for the state of a single-mode of radiation, the so called *Homodyne Tomography*, and thereafter it has been generalized to any quantum system. The basis of the method is just performing measurements of a suitably complete set of observables called *quorum*. For our needs, we just have to measure jointly a quorum of observables, here the spin observables  $\sigma_i$  ( $i = 0, 1, 2, 3$ ), on the two entangled systems at the output, in order to determine the output state  $R_{\text{out}}$ , and hence the quantum operation  $E$ .

In this paper we present the first complete experimental characterization of a quantum device, which in our case will be a single-qubit device. The qubit is encoded on polarization of single photons in the following way

$$|0\rangle = |1\rangle_h |0\rangle_v, \quad |1\rangle = |0\rangle_h |1\rangle_v \quad (4)$$

namely with the “logical zero” state corresponding to a single horizontally polarized photon and the “logical one” state corresponding to a single vertically polarized photon. In the following we will denote by  $h$  and  $v$  the annihilation operators of the horizontally and vertically polarized modes of radiation associated to a fixed wave-vector,  $\mathbf{k}$ . Using single photon states we encode a qubit on the polarization. In the polarization representation, the Pauli matrices write as follows:

$$\begin{aligned} \sigma_1 &= h^\dagger v + v^\dagger h \\ \sigma_2 &= i(h^\dagger v - v^\dagger h) \\ \sigma_3 &= h^\dagger h - v^\dagger v \end{aligned} \quad (5)$$

The ring of Pauli matrices is completed by including the identity  $\sigma_0 = h^\dagger h + v^\dagger v$ . In the following we will denote by  $\vec{\sigma}$  the column three-vector of operators  $\vec{\sigma} = (\sigma_1, \sigma_2, \sigma_3)$ , and by  $\sigma$  the column tetra-vector  $\sigma = (\sigma_0, \sigma_1, \sigma_2, \sigma_3)$ , and use Greek indices for three-vectors components  $\alpha = 1, 2, 3$  (or  $\alpha = x, y, z$ ), and Latin indices for tetra-vector components:  $i = 0, 1, 2, 3$ .

A wave-plate changes the two radiation modes according to the matrix transformation:

$$\begin{pmatrix} h \\ v \end{pmatrix} \longrightarrow w(\phi, \theta)^\dagger \begin{pmatrix} h \\ v \end{pmatrix} w(\phi, \theta) \equiv W(\phi, \theta) \begin{pmatrix} h \\ v \end{pmatrix} \quad (6)$$

where the matrix  $W(\phi, \theta)$  is given by:

$$\begin{aligned} W(\phi, \theta) &= \begin{pmatrix} \cos \theta & -\sin \theta \\ \sin \theta & \cos \theta \end{pmatrix} \begin{pmatrix} 1 & 0 \\ 0 & e^{i\phi} \end{pmatrix} \begin{pmatrix} \cos \theta & \sin \theta \\ -\sin \theta & \cos \theta \end{pmatrix} \\ &= \begin{pmatrix} z_+ + cz_- & sz_- \\ sz_- & z_+ - cz_- \end{pmatrix} \end{aligned} \quad (7)$$

where  $s = \sin 2\theta$ ,  $c = \cos 2\theta$ ,  $\theta$  is the wave-plate orientation angle around the wave-vector  $\mathbf{k}$ ,  $z_\pm = \frac{1}{2}(1 \pm e^{i\phi})$ ,  $\phi = \frac{2\pi\delta}{\lambda}$ ,  $\lambda$  is the wave-length and  $\delta$  is the optical path through the plate. Special cases are the  $\frac{\lambda}{4}$  plate which can be used with  $\theta = \frac{\pi}{4}$  to give the right and left circularly polarized *modes*

$$\begin{pmatrix} r \\ l \end{pmatrix} = W\left(\frac{\pi}{2}, \frac{\pi}{4}\right) \begin{pmatrix} h \\ v \end{pmatrix} = \frac{e^{i\pi/4}}{\sqrt{2}} \begin{pmatrix} h + iv \\ -ih + v \end{pmatrix} \quad (8)$$

and the  $\frac{\lambda}{2}$  plate which can be used to give the diagonal linearly polarized *modes*

$$\begin{pmatrix} a \\ b \end{pmatrix} = W\left(\pi, \frac{\pi}{8}\right) \begin{pmatrix} h \\ v \end{pmatrix} = \frac{1}{\sqrt{2}} \begin{pmatrix} h + v \\ h - v \end{pmatrix}. \quad (9)$$

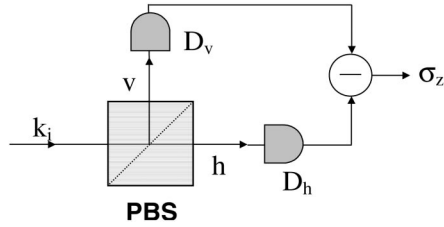


**Fig. 2** Pauli-matrix measurement apparatus for photon polarization qubits inserted at the end of each test optical beam.

The Heisenberg picture evolution of the Pauli matrices corresponding to the unitary  $U$  on the qubit Hilbert space will be given by a rotation, which we will denote as follows

$$U^\dagger \vec{\sigma} U = R(U) \vec{\sigma}. \tag{10}$$

In particular, for a  $\phi$ -wave-plate we have the rotation matrix

$$R(W(\phi, \theta)) = \begin{pmatrix} s^2 + c^2 \cos \phi & -c \cos \phi & sc(1 - \cos \phi) \\ c \sin \phi & \cos \phi & -s \sin \phi \\ sc(1 - \cos \phi) & s \sin \phi & c^2 + s^2 \cos \phi \end{pmatrix}. \tag{11}$$

In particular, for a  $\frac{\lambda}{2}$ -wave-plate we have

$$W(\pi, \theta) = \begin{pmatrix} \cos 2\theta & \sin 2\theta \\ \sin 2\theta & -\cos 2\theta \end{pmatrix} \tag{12}$$

$$R(\pi, \theta) = \begin{pmatrix} -\cos 4\theta & 0 & \sin 4\theta \\ 0 & -1 & 0 \\ \sin 4\theta & 0 & \cos 4\theta \end{pmatrix}.$$

The  $\sigma_z$ -photo-detector is achieved as in Fig. 2. From Eq. (11) we can see that a  $\sigma_x$ -detector can be obtained by preceding the  $\sigma_z$ -detector with a  $\lambda/2$ -wave-plate oriented at  $\theta = \pi/8$ , whereas a  $\sigma_y$ -detector is obtained by preceding the  $\sigma_z$ -detector with a  $\lambda/4$ -wave-plate oriented at  $\theta = \pi/4$ . When collecting data at a  $\sigma_\alpha$ -detector, we will denote by  $\sigma_\alpha = \pm 1$  the random outcome, with  $\sigma_\alpha = \pm 1$  corresponding to the h-detector flashing, and  $\sigma_\alpha = -1$  corresponding to the v-detector flashing instead. The experimental averages for the complete setup must coincide with the following theoretical expectation values

$$\overline{s_i^{(1)} s_j^{(2)}} = \langle \langle \Psi | (U^\dagger \otimes I) (\sigma_i^{(1)} \otimes \sigma_j^{(2)}) (U \otimes I) | \Psi \rangle \rangle \tag{13}$$

and, in particular,  $\overline{s_i^{(1)}} \equiv \overline{s_i^{(1)} s_0^{(2)}}$  and  $\overline{s_i^{(2)}} \equiv \overline{s_0^{(1)} s_i^{(2)}}$  now  $s_i^{(n)}$  denoting the random outcome of the detector of the  $n$ th beam ( $n = 1, 2$ ) in the entangled state. For maximally entangled states we have also  $\overline{s_\alpha^{(1)}} = \overline{s_\alpha^{(2)}} = 0$  for all  $\alpha = x, y, z$ . The theoretical expectations for the setup without the device to be characterized are given by:

$$\langle \langle \Psi | (\sigma_i^{(1)} \otimes \sigma_j^{(2)}) | \Psi \rangle \rangle = \text{Tr} \left[ \Psi^\dagger \sigma_i \Psi \sigma_j^* \right], \tag{14}$$

where  $\Psi$  denotes the matrix of the state on the customary basis of eigenvectors of  $\sigma_z$ . In particular, for the four Bell states

$$\frac{1}{\sqrt{2}} | \sigma_j \rangle \rangle = \sigma_j \otimes I \frac{1}{\sqrt{2}} | I \rangle \rangle \tag{15}$$

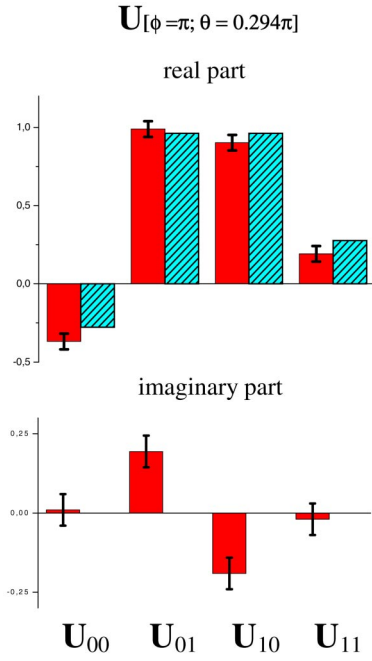


**Fig. 3** (online colour at: [www.interscience.wiley.com](http://www.interscience.wiley.com)) Experimental characterization by Pauli Tomography of a single optical  $\lambda/2$  Waveplate [ $\varphi = \pi; \theta = +0.249\pi$ ] inserted on channel  $\mathbf{k}_1$  with the following optical properties: retardation phase  $\varphi = (\pi)$ ; orientation angle of the optical axis respect to the laboratory horizontal direction “h”:  $\theta = (0.249\pi)$ . The experimental real and imaginary parts of the four matrix elements  $U_{ij}$  of the Waveplate are shown together with the related measured statistical variances. The corresponding theoretical values are shown for comparison.

we have

$$\frac{1}{\sqrt{2}}\Delta_{ij}(\sigma_k) = \delta_{ij}H_{kj}, \quad H = \begin{bmatrix} 1 & 1 & -1 & 1 \\ 1 & 1 & 1 & -1 \\ 1 & -1 & -1 & 1 \\ 1 & -1 & 1 & 1 \end{bmatrix}. \quad (16)$$

Using Eq. (10) and (14) we obtain

$$\overline{s_\alpha^1 s_\beta^2} = \sum_\lambda R_{\alpha\lambda}(U)\Delta_{\lambda\beta}(\Psi). \quad (17)$$

In particular, in the lab we use the multiplet state corresponding to  $\Psi = \sigma_x/\sqrt{2}$ , whence we have

$$\overline{s_\alpha^1 s_\beta^2} = R_{\alpha\beta}(U)\Delta_{1\beta}(\Psi).$$

### 3 Method, apparatus and results

The input maximally entangled state  $|\Psi\rangle\rangle$ , expressed by Eq. (2), was SPDC generated in the laboratory by an optical parametric amplifier (OPA) physically consisting of a nonlinear (NL) BBO ( $\beta$ -barium-borate) crystal plate, 2 mm thick, cut for Type II phase matching and excited by a pulsed mode-locked ultraviolet laser UV having pulse duration  $\tau = 140$  fsec and wavelength (wl)  $\lambda_p = 397.5$  nm. Precisely, the apparatus was set to generate on the two modes  $\mathbf{k}_i$ , i.e. the entangled systems  $i = 1, 2$ , single photon couples in a polarization entangled “triplet” state, viz.  $|\Psi\rangle\rangle = 2^{-1/2}|\sigma_x\rangle\rangle$ , according to Eq. (15). The wl of the emitted photons was  $\lambda = 795$  nm. The measurement apparatus consisted of two equal polarizing beam splitters  $PBS_i$  with output modes coupled to four equal Si-avalanche photo-detectors SPCM-AQR14 with quantum efficiencies  $QE \simeq 0.42$ . The beams exciting the detectors were filtered by equal interference filters within a bandwidth  $\Delta\lambda = 6$  nm. The detector output signals were finally analyzed by a computer. We want now

$$\mathbf{U}''_{[\varphi=\pi, \theta=0.294\pi]} \times \mathbf{U}'_{[\varphi=0.45\pi, \theta=-0.139\pi]}$$

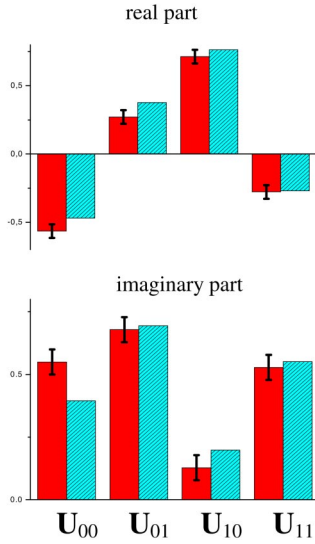


**Fig. 4** (online colour at: [www.interscience.wiley.com](http://www.interscience.wiley.com)) Experimental Characterization by Pauli Tomography of a combination of two optical Waveplates: the Waveplate  $[\varphi = 0.45\pi; \theta = -0.138\pi]$  (cf. Fig. 3) followed by a  $\lambda/2$  Waveplate  $[\varphi = \pi; \theta = +0.29\pi]$ . The experimental real and imaginary parts of the four matrix elements  $U_{ij}$  of the combination are shown together with the related measured statistical variances. The corresponding theoretical values are shown for comparison.

to determine experimentally by this apparatus the matrix elements of the state  $|\Psi\rangle\rangle$  expressed by Eq. (2). This can be achieved as follows: from the trivial identity

$$\langle nm | \Psi \rangle\rangle = \Psi_{nm}, \tag{18}$$

we obtain the matrix  $\Psi_{nm}$  for the *input states* in terms of the following ensemble averages

$$\Psi_{nm} = e^{i\varphi} \frac{\langle\langle \Psi | 01 \rangle\rangle \langle nm | \Psi \rangle\rangle}{\sqrt{\langle\langle \Psi | 01 \rangle\rangle \langle 01 | \Psi \rangle\rangle}} \tag{19}$$

where the unmeasurable phase factor is given by:  $\exp(i\varphi) = \Psi_{01}/|\Psi_{01}|$ . The choice of the vector  $|01\rangle$  is arbitrary as it is needed only for the sake of normalization: e.g. we could have used  $|10\rangle$  or  $|11\rangle$ , instead. Using the *tomographic expansion* over the four Pauli matrices [3], [4] we see that, in virtue of Eq. (19), the matrix element of the input state is obtained from the following experimental averages:

$$\Psi_{nm} = \frac{1}{4\sqrt{p}} \sum_{ij} Q_{ij}(nm) \overline{s_i^{(1)} s_j^{(2)}}, \tag{20}$$

where

$$p = \langle\langle \Psi | 01 \rangle\rangle \langle 01 | \Psi \rangle\rangle = \frac{1}{4} \left(1 + s_3^{(1)}\right) \left(1 - s_3^{(2)}\right) \tag{21}$$

is the fraction of coincidences with both  $\sigma_z$ -detectors firing on h, and the matrix  $Q(nm)$  is given by

$$Q_{ij}(nm) = \langle n | \sigma_i | 0 \rangle \langle m | \sigma_j | 1 \rangle \tag{22}$$

the unitary matrix  $U_{nm}$  of the device is now obtained with the same averaging above but now for the state at the output of the device:  $|U\Psi\rangle\rangle = (U \otimes I) |\Psi\rangle\rangle$ . Therefore, we now have:

$$(U\Psi)_{nm} = e^{i\varphi} \frac{\langle\langle U\Psi | 01 \rangle\rangle \langle nm | \Psi U \rangle\rangle}{\sqrt{\langle\langle U\Psi | 01 \rangle\rangle \langle 01 | \Psi U \rangle\rangle}}, \tag{23}$$

where we use again Eqs. (21), (22), but now the average expressed by 20 is carried out over the output state  $|U\Psi\rangle$ . The (complex) parameters  $U_{nm}$  are obtained from Eq. (23) by matrix inversion. This is of course possible since the matrix  $\Psi$  is invertible, in virtue of the entangled character of  $|\Psi\rangle$ .

The experimental demonstration of the tomographic process is given in Figs. 3 and 4 where both *real* and *imaginary parts* of the four components of the matrix  $U$  are reported for two different “unknown” devices inserted in the mode  $k_1$  of the tomographic apparatus. The experimental results are shown together with the corresponding data evaluated theoretically. Furthermore the experimental “variance” of the data are also reported. Each “unknown” device is represented in one figure, namely:

**Fig. 3:** a single  $\lambda/2$  Waveplate [ $\varphi = \pi; \theta = +0.249\pi$ ] i.e., with retardation phase  $\varphi = (\pi)$  and orientation angle respect to the “horizontal” direction “h” :  $\theta = (0.249\pi)$ .

**Fig. 4:** a combination of 2 Waveplates: i.e. a Waveplate [ $\varphi = 0.45\pi; \theta = -0.138\pi$ ] followed by a  $\lambda/2$  Waveplate [ $\varphi = \pi; \theta = +0.29\pi$ ].

As we may see, the experimental results are found in good agreement with theory.

## 4 Conclusions

We have given the first demonstration, in a simple single-qubit context, of a novel Tomographic method which is able to fully characterize the properties of any device acting on a quantum system by exploiting for the first time the complete intrinsic parallelism of the quantum entanglement. This method establishes a new fundamental framework of utterly paradigmatic relevance in the domains of modern Quantum Measurement theory and Quantum Information.

Our method is expected to be of general and far reaching relevance. In facts, it can be adopted within more general and complex multi-qubit systems. For instance by this method a full characterization of a two-qubits device, such as a controlled-NOT, can be achieved. In this case we just need to double the input and the measurement setup, by providing two input entangled states and four detectors coupled at the outputs of the two pairs of the device channels. The full quantum characterization of the the device is finally obtained by a joint tomographic reconstruction on both channels of the device.

**Acknowledgements** We are indebted with the FET European Network on Quantum Information and Communication (Contract IST-2000-29681-ATESIT), the I.N.F.M. PRA 2001 “clon” and with M.U.R.S.T. for funding.

## References

- [1] I. L. Chuang and M. A. Nielsen, Quantum Information and Quantum Computation (Cambridge University Press, Cambridge 2000).
- [2] K. Kraus, States, Effects, and Operations (Springer-Verlag, Berlin 1983).
- [3] G. M. D’Ariano, Quantum Tomography, Proceedings of the Intl. School “E. Fermi”, Varenna: Experimental Quantum Computation and Information, edited by F. De Martini and C. Monroe (Editrice Compositori, Bologna 2001).
- [4] G. M. D’Ariano and P. Lo Presti, Tomography of quantum operations, Phys. Rev. Lett. **86**, 4195 (2001).
- [5] W. K. Wootters and W. H. Zurek, A single quantum cannot be cloned, Nature (London) **299**, 802 (1982).
- [6] G. M. D’Ariano and H. P. Yuen, On the impossibility of measuring the wave function of a single quantum system, Phys. Rev. Lett. **76**, 2832 (1996).